JOURNAL OF OPTOELECTRONICS AND ADVANCED MATERIALS Vol. 10, No. 11, November 2008, p. 3022 - 3028

Picosecond laser system based on microchip oscillator

A. STRATAN, L. RUSEN*, R. DABU, C. FENIC, C. BLANARU
Department of Lasers, National Institute for Laser, Plasma, and Radiation Physics, 409 Atomistilor St., PO Box MG-36, 077125 Bucharest, Romania

We have developed a high-energy, compact, picosecond laser consisting of a diode-pumped, passively Q-switched microchip laser, and a flash-pumped two-pass Nd:YAG amplifier. Amplified pulses of maximum 19-mJ energy, 460-ps duration at (1-10) Hz rate, in a nearly TEM_{00} transversal mode at 1064-nm wavelength, were obtained. The infrared pulses were nonlinearly converted to 532-nm second harmonic and 266-nm fourth harmonic with a conversion efficiency of 50 % and 20 %, respectively.

(Received August 2, 2008; accepted October 30, 2008)

Keywords: Picosecond pulses, Microchip laser, Flash-pumped amplifier, Second harmonic, Fourth harmonic

1. Introduction

Pulsed solid-state lasers are widely used in scientific, medical, industrial and military applications. In some key applications, energetic short pulses (< 1 ns) can bring significant advantages. For example, in ranging, 3D imaging, high-speed/strobe photography, and in scientific"excite and probe" type experiments they allow increased temporal or spatial resolution. In the case of precision micro-machining there is practical evidence that they allow results of superior quality due to the much reduced heat diffusion into the bulk material [1, 2].

Mode-locked lasers and electrooptically Q-switched stimulated Brillouin scattering (SBS)-compressed Nd:YAG lasers offer high-energy (tens–hundreds millijoules) picosecond pulses, but these laser systems are sophisticated, large-size and expensive devices, suited mainly for laboratory use [3, 4]. For applications in ranging, LIDAR, sensing, and material micro-processing, compact and efficient laser systems with short pulses are required. Diode-pumped, passively Q-switched microchip lasers are all-solid-state sources of short pulses, with good TEM_{00} beam quality and high repetition-rate from a compact package. These devices provide only a moderate energy per pulse, from few microjoules to millijoules [5, 6, 7].

We report here a high-energy, compact, picosecond laser system consisting of a diode-pumped, passively Q-switched microchip laser, as an oscillator-seed, and a flash-pumped Nd:YAG amplifier. For high energy amplifiers, the flashlamp pumping still remains a simple and cost effective solution comparing to the diode laser pumping due to the capability to deliver high-power density pump pulses. The laser generates up to 19-mJ infrared-pulses of 460 ps duration at maximum 10-Hz rate, in a nearly TEM_{00} Gaussian mode. Due to the efficient nonlinear conversion of the infrared output, energetic short pulses (< 400 ps) in visible (532 nm) and UV (266 nm) are also available.

2. Laser set-up

The microchip laser used in our set-up consists in a thin disk of a 1.1%-doped Nd:YAG active medium diffusion bonded to a thin piece of Cr:YAG crystal, used as saturable absorber. The outer faces of the microchip are polished for laser mirror quality, with 5 arc-seconds precision of the parallelism. The 810-nm pump-beam of a laser diode was coupled to the microchip laser through a 100-μm diameter fiber and a 1:1 imaging optics (Fig. 1). When pumped by 1-W average power pulsed radiation, the microchip generated 8.6-μJ energy pulses of ~ 460-ps FWHM duration at a pulse repetition rate of 1 kHz in a nearly TEM_{00} transversal mode (beam quality factor, $M^2 \approx 1.1$). The microchip output of 1064-nm wavelength was linearly polarized with a contrast higher than 100:1. Microchip laser was placed in the focal plane of the beam expanding lens, EL. The polarization plane of the microchip laser radiation was adjusted by a λ/2 waveplate, WP. The microchip output is amplified up to 19-mJ pulse-energy in a two-pass amplifier that consists in a flash-pumped Nd:YAG rod, 5-mm diameter, 100-mm long. To prevent feedback and prelasing, the rod ends are cut at a small oblique angle and coated with antireflection layers. The collimated beam is directed through the amplifier by the M1-M4 high reflecting mirrors at 1064 nm wavelength. Due to the high amplification factor, optical isolation between microchip oscillator and laser amplifier was necessary. The amplifier output was 1.6x collimated using a beam expander, in order to reduce the beam power density in the frequency-conversion stages. After the second harmonic (SH) generation in a LBO frequency-doubling crystal, the green output is extracted with dichroic mirrors M7, MF2 (flipping mirror), HR at 532 nm. The SH beam is directed through the frequency-quadrupling crystal by the green separators M7, M8, and the UV output is extracted using the UV separators M9 and M10, HR at 266 nm. The useless laser radiation is suppressed into dumpers D1, D2.

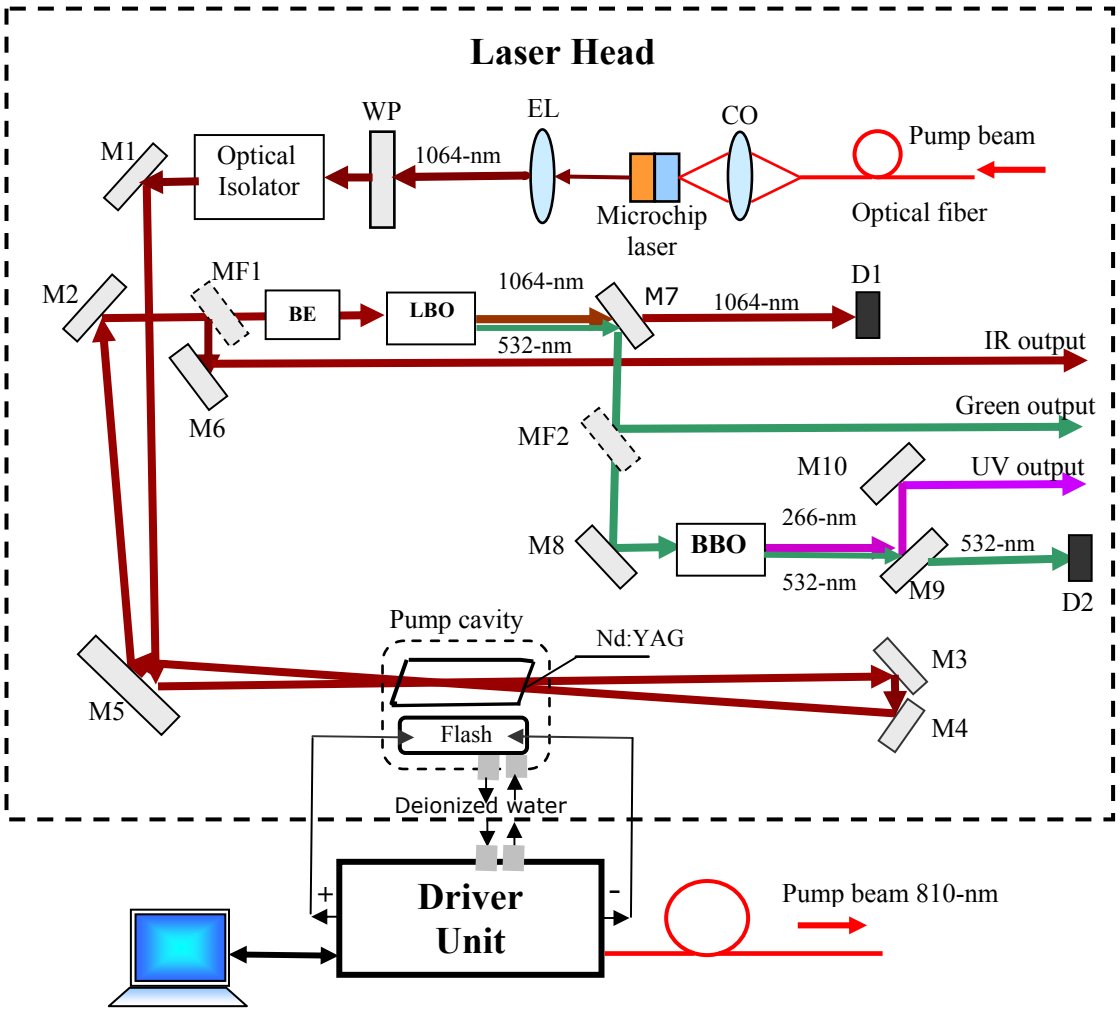

Fig. 1 Schematic of microchip oscillator–amplifier laser system. CO: collimating/focusing optics; EL: expanding lens; WP: λ/2 waveplate; M1-M6: highly reflective (HR) mirrors at 1064 nm; MF1: flipping mirror, HR at 1064 nm; M7-M8,: dichroic mirrors (green separators); MF2: dichroic flipping mirror, HR at 532 nm, high transmission at 1064 nm; BE: 1.6x beam expander; LBO: frequency-doubling crystal; BBO: frequency-quadrupling crystal; M9-M10: dichroic mirrors (UV separators). D1-D2: dumpers; Nd:YAG: amplifier rod.

A dedicated software synchronizes the flash-pumped Nd:YAG amplifier with the microchip laser pulses, and sets / monitors the operating / status parameters of the system. The laser system generates an output pulse for each discharge shot applied to the flashlamp.

The whole laser system consists of a laser head having 500 x 300 x 120 mm size and a driver unit (including cooling unit) of 525 x 395 x 480 mm. The driver unit provides an average pump-power of max. 1000 W at 10-Hz flash-shot repetition rate.

3. Results and discussion

Because of the variation of the pulse beam radius between the passes through the Nd:YAG rod, we evaluated the total amplifier gain in two steps, for the first pass and the second pass. In order to calculate the pulse-energy that can be extracted from the two-pass amplifier, we measured the single pass energy-gain for different low-input fluences F_{in}, much smaller than the saturation fluence F_s of the Nd:YAG.

$$F_s = h\nu / \sigma = 0.66\ J/cm^2\ ,$$

where $\sigma = 2.8 \times 10^{-19}\ cm^2$ is the stimulated emission cross section of Nd:YAG [8], and $h\nu = 1.86 \times 19^{-19}\ J$ is the photon energy at 1064-nm wavelength. The single-pass gain was measured by using a high-sensitive pyroelectric detector placed 10-cm distant from the end of Nd:YAG rod. The contribution of the flash output to the measured pulse energy was subtracted from the measured data. In Fig. 2 we plot the measured single pass gain versus pump energy of the flashlamp, for three input levels. Without input attenuation (input pulse energy $E_{in}^{(1)} = 8.6\,\mu J$ and input average fluence $F_{in} = 9 \times 10^{-4}\ J/cm^2$), for *50-J* pump

energy, an output pulse energy of 0.76 mJ was measured, corresponding to a single-pass gain $G_1 \approx 88$. The small-signal gain, G_0, was considered the single-pass gain measured for the lowest input fluence ($F_{in} = 4.5 \times 10^{-5}$ J/cm^2, $F_{in}G_0 << F_s$) obtained by 20 times attenuation of the 8.6-μJ microchip pulse energy.

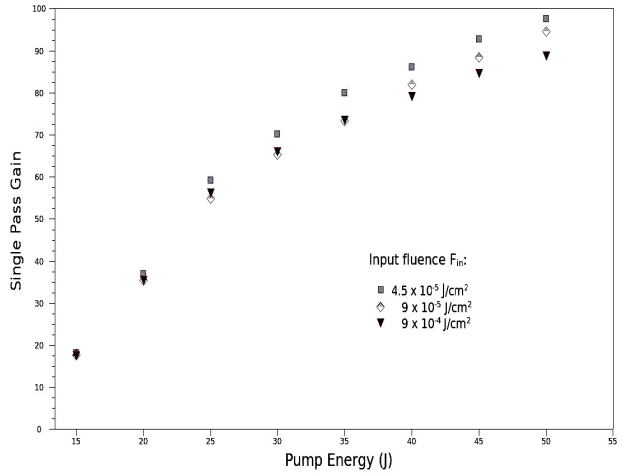

Fig. 2. Single-pass gain as a function of the pump energy.

As shown in Fig. 2, even for the lowest input, the single pass gain as a function of flash pump changes from an exponential (small-signal) relationship to a linear (saturated) relationship for more than 25-J pump energy. We measured a small-signal gain G_0 of 60 at 25-J pump energy, which allows us to calculate the corresponding inverted population density n according to [9]

$$G_0 = \exp(n\sigma l) \tag{1}$$

where $l = 10$ cm is the length of the Nd:YAG rod. The resulting inverted population $n = 1.46 \times 10^{18}$ cm^{-3} is negligible in comparison to the ground level population of 1.38×10^{20} cm^{-3}. The depletion of the ground level population is not significantly involved in the saturation of single pass gain. According to (1) and Fig. 2, the saturation of the small signal gain for 25-50 J pump energy implies that the inverted population n does not increase linearly with the increase of the pump energy. Amplified spontaneous emission (ASE) and parasitic oscillations due to the high-gain properties of the Nd:YAG effectively can limit the energy storage density and therefore the useful energy which can be extracted for a given rod. ASE is a process which will be enhanced by radiation from the flashlamp falling within the wavelength of the laser transition, or by an increase of the path-length in the gain medium either by internal or external reflection. A threshold for ASE does not exist, however, the emitted fluorescence increases rapidly with gain [9].

For a uniform distribution of the input fluence F_0 and pump energy inside the amplifying medium, the output fluence F_{out} is given by [9]:

$$F_{out} = F_s \ln\left\{1 + \left[\exp\left(\frac{F_0}{F_s}\right) - 1\right] G_0\right\} \tag{2}$$

Assuming a Gaussian distribution of the input pulse intensity and a uniform distribution of the pump energy inside the laser rod, we have calculated the pulse energy, $E_{out}^{(2)}$, after the second-pass amplification by integrating the output fluence over the beam area using the following equation:

$$E_{out}^{(2)} = F_s \int_0^{kw_2} \int_0^{2\pi} \ln\left\{1 + \left(\exp\left[\frac{2E_{in}^{(2)}}{\pi w_2^2 F_s}\exp\left(-\frac{2r^2}{w_2^2}\right)\right] - 1\right) G_0\right\} r\, dr\, d\theta \tag{3}$$

where $E_{in}^{(2)} = E_{out}^{(1)} = E_{in}^{(1)} G_1$ is the energy of the first pass amplified pulse, w_2 is the beam radius for the second pass, $k \approx 1.1$ is a factor given by the geometry of the laser amplifier. The values of the laser parameters used in our calculations are shown in Table 1.

Table 1. Parameters of the Nd:YAG amplifier.

Laser parameter	Value
Saturation fluence of Nd:YAG	$F_s = 0.66$ J/ cm^2
Length of the Nd:YAG rod	$l = 10$ cm
Pulse-energy injected into two-pass amplifier	$E_{in}^{(1)} = 8.6\ \mu J$
Single-pass gain G_0	18 – 97 for 15-50 J pumpinput, as shown in Fig. 2
Beam radius for the first pass	$w_1 = 0.55$ mm
Beam radius for the second pass	$w_2 = 0.6$ mm

The calculation results and the measured values are shown in Fig. 3, which represents the energy extracted from the two-pass amplifier versus flash pump. The measured and calculated second pass gain G_2 versus pump energy is shown in the Fig. 4. For the second pass gain, we noticed a saturation of the amplification due to the fluence pulse increase up to a significant value compared to the Nd:YAG saturation fluence. The two-pass amplified pulse energy was restricted by the damage threshold of the M_2 and M_5 mirrors. For 50-J pump energy, an overall two-pass amplifier gain as high as 2200 was measured.

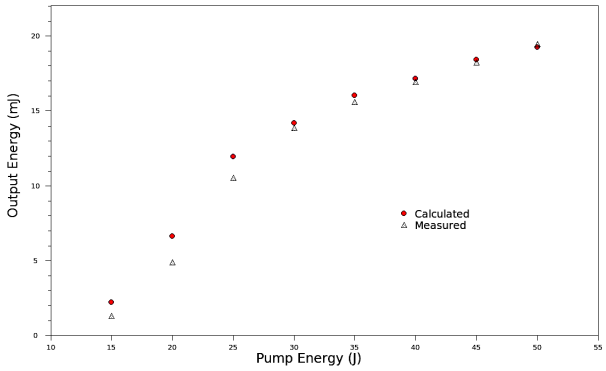

Fig. 3 Pulse energy extracted from the double-pass amplifier.

In order to minimize the power consumption required to achieve a given amplifier gain, the discharge circuit of the flashlamp has to be optimized both from the electrical and the spectral point of view. Normally, a critically damped discharge circuit is desired (i.e. the damping parameter, $\alpha \approx 0.8$). So the maximum electrical energy is converted into the flash light in the shortest time without undershoot. Furthermore, the pumping efficiency depends to a great extent upon the spectral distribution of light emitted by the flashlamp. The spectral output of a xenon flashlamp depends upon the ratio of discharge energy to the product of pump pulse duration and surface area of the flash envelope. This is the E_d / TA ratio, where E_d is discharge energy, T is the flash-current pulse width, A is the cross sectional area of the lamp [10]. When pumping Nd;YAG, the optimum pump-power density is achieved with E_d / TA ratios in the neighborhood of 16000 W/cm^2. In this range of power density, the emissivity between 700 nm and 900 nm (the spectral region where Nd:YAG has its greatest absorption) is close to one. At Ed / TA ratios lower or higher than 16000 W/cm^2, the black body peak is enlarged or moved to shorter wavelengths, respectively [11, 12]. In our set-up, the optimum discharge regime is achieved for the pump-energy range of 50 – 55 J, where the damping parameter α and the Ed / TA ratio are in the neighborhood of 0.8 and 16000 W/cm^2, respectively.

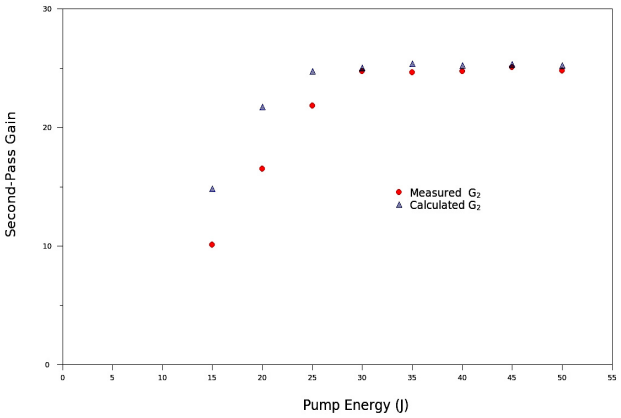

Fig. 4. Measured and calculated second-pass gain G_2 versus pump energy.

The amplifier output preserves the quasi-TEM$_{oo}$ intensity profile of the microchip pulse injected in the amplifier, as shown in Figure 5. We measured the beam quality factor of the amplified infrared pulses, $M^2 < 1.3$, on both horizontal and vertical planes.

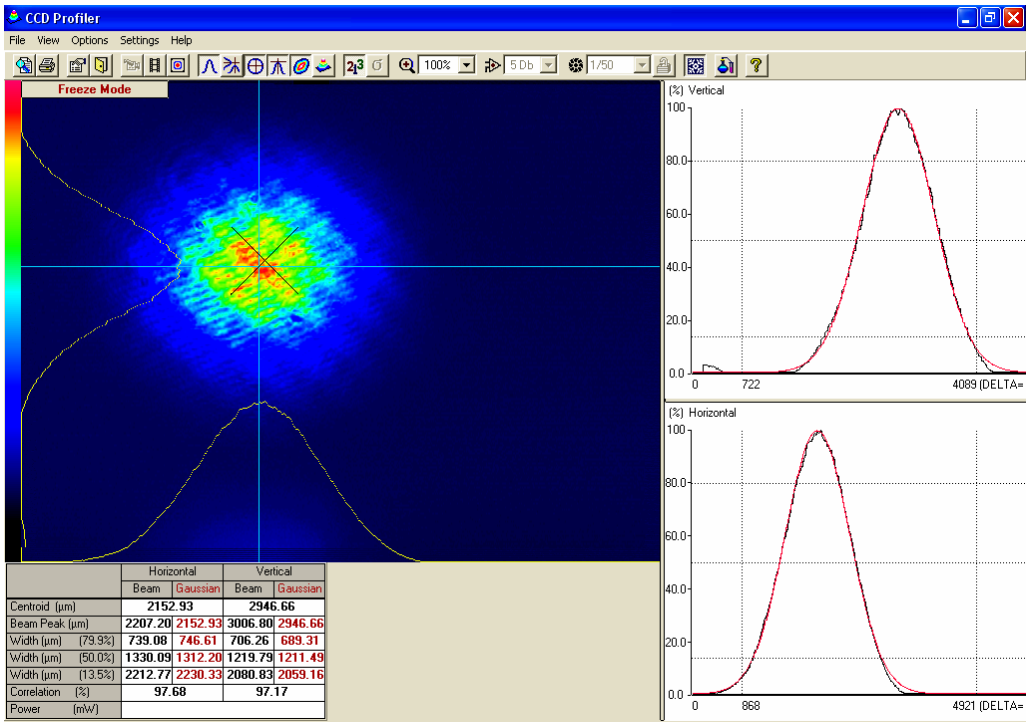

Fig. 5. Transversal intensity profile of the infrared output: 15-mJ pulse energy, 2-Hz pulse repetition rate.

The full-width half-maxim (FWHM) duration of the amplified laser pulse was measured using a fast photodiode D400FC (1-GHz frequency bandwidth) fiber coupled to a Tektronix DPO 7354 digital oscilloscope of 3.5-GHZ bandwidth, with the result shown in Figure 6. Due to limited bandwidth of the photodiode and oscilloscope, it is necessary to operate a rise-time correction [13, 14]. To estimate the actual FWHM duration of the laser pulse, we used the equation

$$\tau^2_{puls-mas} = \tau^2_{puls} + \tau^2_{osc} + \tau^2_{ph} \quad (4)$$

where $\tau_{puls-mas}$= 587 ps is the displayed FWHM pulse duration, the oscilloscope rise-time $\tau_{osc} \approx$ 100 ps, the photodiode rise time $\tau_{ph} \approx$ 350 ps, τ_{puls} the actual FWHM pulse duration. From (1) we obtained the FWHM duration of the infrared output pulse, $\tau_{puls} \approx$ 460 ps.

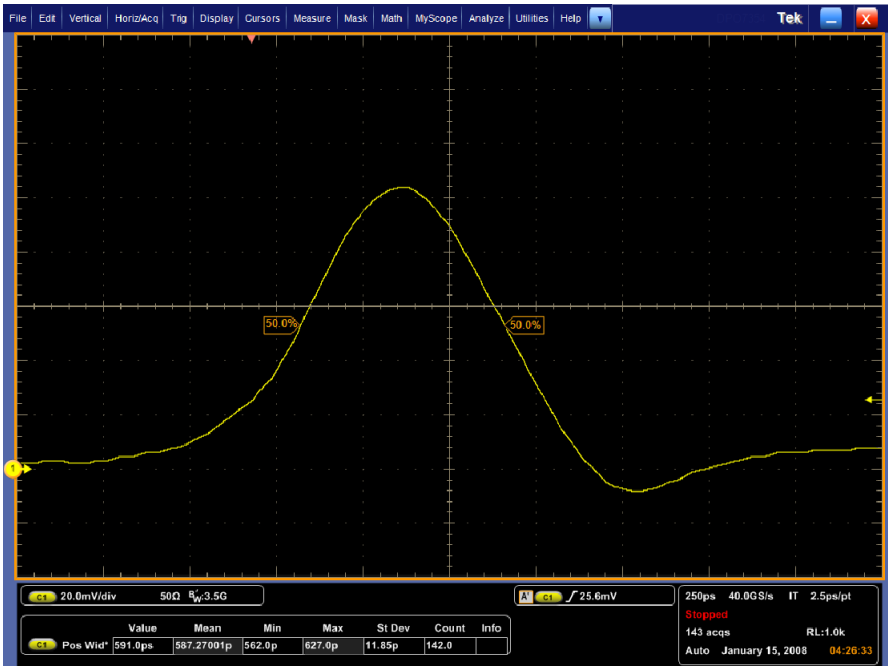

Fig. 6. Temporal profile of the infrared output. Actual FWHM duration (after rise-time correction): ~460-ps.

For second harmonic (SH) generation we used a type I room-temperature critically-phase-matched LBO crystal ($\theta = 90^0$, $\varphi = 11.3^0$), 5 x 5 x 15 mm size. For fourth harmonic (FH) generation at 266 nm, a type I room-temperature critically-phase-matched BBO crystal ($\theta = 90^0$, $\varphi = 47.6^0$), 5 x 5 x 7 mm size, was used. For 19-mJ

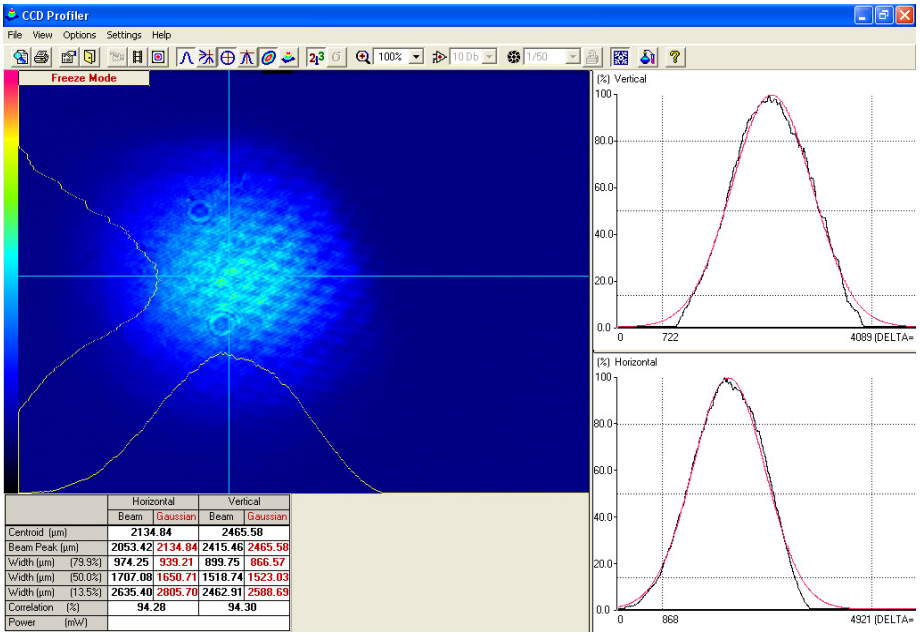

Fig. 7. Transversal intensity profile of the SH output; 7-mJ pulse energy, 2-Hz pulse rate.

amplified infrared pulses, the output pulse-energy of SH and FH was ~ 9.5 mJ and 3.8 mJ, respectively, which corresponds to 50% and 20% conversion efficiency.

The Gaussian profile of the infrared pulse is well preserved by the SH output, as shown in Fig. 7.

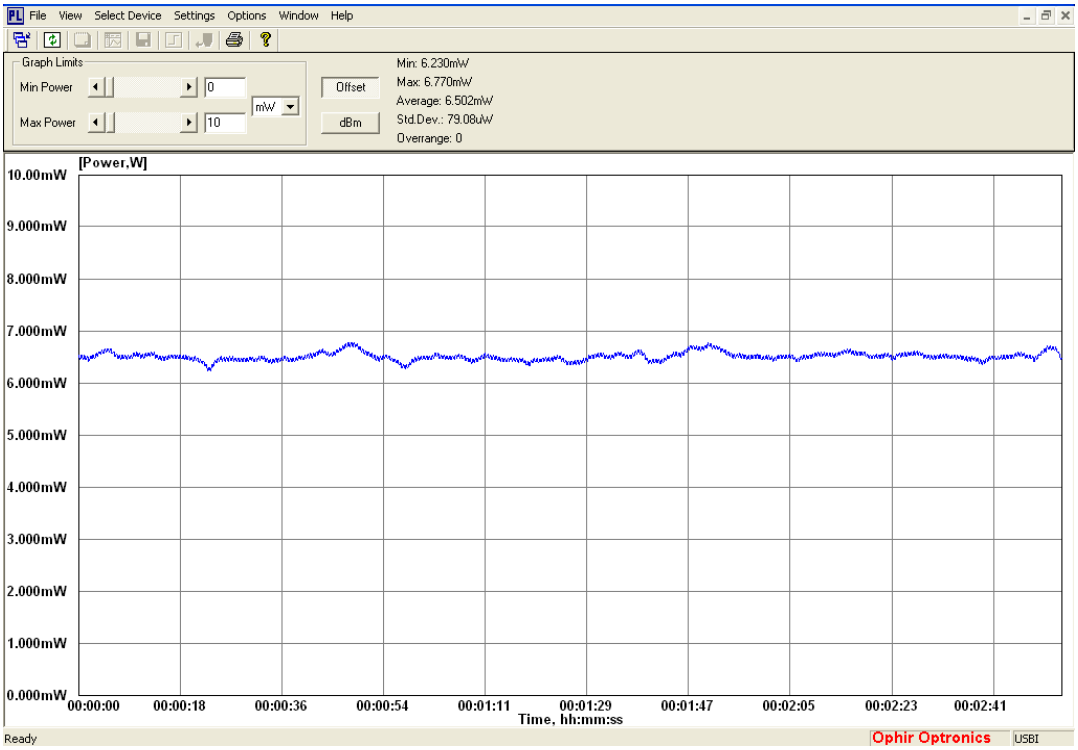

Fig. 8. Evolution of UV output power (266-nm): pulse energy 3.2-mJ, pulse rate 2-Hz, rms <1.3 %.

The short-term stability of the UV output at 266-nm wavelength is shown in Fig. 8. Over 3 minutes we measured a rms value of 1.3 % for 3.2-mJ pulse-energy and 2-Hz pulse repetition rate.

4. Conclusions

We have built a picosecond laser system consisting of a diode-pumped microchip oscillator-seed and a high gain double-pass flash-pumped Nd:YAG amplifier. A total gain higher than 2200 was measured for the highest 50-J pump energy of the amplifier rod. Due to its main features (19-mJ infrared pulse-energy of 460-ps duration with good TEM_{00} beam quality, high conversion efficiency in visible and UV, good pulse energy stability for all generated wavelengths, compactness), the laser system is well suited for precision micro-machining and field applications. To design such a device for a dedicated application, in order to obtain more efficient and small-size laser system, the following improvements could be considered:

i) Increase of the Nd:YAG rod diameter in order to accept a larger input beam diameter and, consequently, to settle a higher energy saturation of the amplified pulses.

ii) Restriction of the Nd:YAG rod length in the 60-75 mm range to reduce ASE.

iii) To set a constant pump energy corresponding to the electrical and spectral optimization of the flash-lamp discharge circuit.

Especially in the case of field applications, it is important to consider the size of the driver unit that strongly depends on the required pulse repetition rate.

In order to obtain output pulses of few-millijoules energy at higher pulse repetition rate (hundreds of Hz), a diode–pumped either bulk or fiber active medium amplifier could be a promising solution.

Acknowledgements

This work was supported by the National Programme CEEX 2005, Project NANOLAS / C39.

References

[1] J. J. Aubert, Laser Focus World, S1, June (1995).
[2] M. Gower, Opto & Laser Europe, **10**, March (2000).
[3] http://www.ekspla.com/en/main/products/17/19?PID=459
[4] http://www.quantel.fr/fr/fiche_produit.php
[5] http://www.alphalas.com/products/lasers/subnanosecond-passively-q-switched-dpss-microchip-lasers-pulselas-p-series.html

[6] J. J. Zayhowski, Opt. Lett. **22**, 169 (1997).
[7] J. J. Zayhowski, Opt. Lett. **21**, 588 (1996).
[8] CASIX Product Catalog (Crystals; Optics; DPO Kits), 2004, p. 113.
[9] W. Koechner, Solid State Laser Engineering, Springer-Verlag, Berlin Heidelberg (1996).
[10] ILC Technology, An overview of flashlamps and CW arc lamps, Technical Bulletin 3 (1986).
[11] J. H. Goncz, Journal of Applied Physics **36**, 742 (1965).
[12] J. L. Emmet, et al, Journal of Applied Physics **35**, 2601 (1964).
[13] http://ess.web.cern.ch/ESS/EquipmentSelectorGuide/Oscilloscopes/risetime.htm
[14] G. E. Valley, Jr. and H. Wallman, Vacuum Tube Amplifiers, MIT Radiation Laboratory Series 18, McGraw-Hill (1948). Retrieved from http://en.wikipedia.org/wiki/Rise_time".

*Corresponding author: laurentiu.rusen@inflpr.ro